Automatica 121 (2020) 109161

Contents lists available at ScienceDirect

Automatica

journal homepage: www.elsevier.com/locate/automatica

Brief paper

Adaptive control allocation for constrained systems☆

Seyed Shahabaldin Tohidi [a,*], Yildiray Yildiz [a], Ilya Kolmanovsky [b]

[a] Mechanical Engineering Department, Bilkent University, Ankara, 06800, Turkey
[b] Department of Aerospace Engineering, University of Michigan, Ann Arbor, MI 48109, USA

ARTICLE INFO

Article history:
Received 2 July 2019
Received in revised form 2 June 2020
Accepted 24 June 2020
Available online 7 August 2020

Keywords:
Control allocation
Uncertain systems
Actuator saturation

ABSTRACT

This paper proposes an adaptive control allocation approach for uncertain over-actuated systems with actuator saturation. The proposed control allocation method does not require uncertainty estimation or persistency of excitation. Actuator constraints are respected by employing the projection algorithm. The stability analysis is provided for two different cases: when ideal adaptive parameters are inside and when they are outside of the projection boundary which is chosen consistently with the actuator saturation limits. Simulation results for the Aerodata Model in Research Environment (ADMIRE), which is used as an example of an over-actuated aircraft system with actuator saturation, demonstrate the effectiveness of the proposed method.

1. Introduction

Control allocation is the process of distributing control signals among redundant actuators which is employed in many engineering domains such as aerial vehicles (Acosta et al., 2014; Bodson, 2002; Ducard, 2009; Liao, Lum, Wang, & Benosman, 2010; Sadeghzadeh, Chamseddine, Zhang, & Theilliol, 2012; Shen, Wang, Zhu, & Poh, 2015, 2017; Tohidi, Yildiz, & Kolmanovsky, 2018; Yildiz & Kolmanovsky, 2011a, 2011b), marine vehicles (Chen, Ge, How, & Choo, 2013; Gierusz & Tomera, 2006; Johansen, Fuglseth, Tøndel, & Fossen, 2008; Podder & Sarkar, 2001; Sørensen, 2011), automobiles (Demirci & Gokasan, 2013; Tjønnås & Johansen, 2010), robots (Taghirad & Bedoustani, 2011), and power systems (Bouarfa, Bodson, & Fadel, 2017; Raoufat, Tomsovic, & Djouadi, 2017). In particular, in aircraft and spacecraft applications, the flight control law determines forces and moments while control actuator settings are determined through control allocation. Control allocation improves fault tolerability and modularity of the overall control system while permitting to exploit actuator redundancy for improved maneuverability.

Control allocation methods can be categorized into the following three categories: Pseudo-inverse-based methods, optimization based methods and dynamic control allocation. Given a mapping between a control input v and the actuator input vector u defined as $Bu = v$, in pseudo inverse based control allocation (Alwi & Edwards, 2008; Durham, 1993; Durham, Bordignon, & Beck, 2009; Tohidi, Khaki Sedigh and Buzorgnia, 2016), the control input is distributed to the individual actuators by the pseudo inverse mapping, i.e., $u = B^{+}v$, which is the minimum 2-norm solution among infinitely many control allocation solutions. Such a method can be extended to account for actuator saturation (Buffington & Enns, 1996; Durham, 1993; Durham et al., 2009; Kirchengast, Steinberger, & Horn, 2018; Stephan & Fichter, 2017; Tohidi, Khaki et al., 2016; Virnig & Bodden, 1994). In optimization based control allocation (Casavola & Garone, 2010; Härkegård, 2002; Härkegård & Glad, 2005; Petersen & Bodson, 2006; Yildiz & Kolmanovsky, 2010; Yildiz, Kolmanovsky, & Acosta, 2011), control allocation is performed by minimizing the cost function $\|Bu - v\| + J_0$, where J_0 represents a secondary objective such as minimizing actuator deflections. For a recent optimization based computationally efficient control allocation example see Yang and Gao (2020). In dynamic control allocation (Falconí & Holzapfel, 2016; Galeani & Sassano, 2018; Tjønnås & Johansen, 2008; Tohidi, Yildiz and Kolmanovsky, 2016; Tohidi, Yildiz, & Kolmanovsky, 2017; Zaccarian, 2009), the control signals are distributed among actuators using a set of rules dictated by differential equations. A survey of control allocation methods can be found in Johansen and Fossen (2013).

Control allocation is an appealing approach also for the design of active fault-tolerant control systems (Argha, Su, & Celler, 2019; Ducard, 2009; Edwards, Lombaerts, Smaili, et al., 2010; Sørensen, Hansen, Breivik, & Blanke, 2017; Zhang & Jiang, 2008).

☆ This work was supported by the Scientific and Technological Research Council of Turkey under grant number 118E202, and by Turkish Academy of Sciences the Young Scientist Award Program. The material in this paper was presented at: the 2016 American Control Conference, July 6–8, 2016, Boston, MA, USA. the 20th IFAC World Congress of the International Federation of Automatic Control, July 9–14, 2017, Toulouse, France. the 2nd IEEE Conference on Control Technology and Applications, August 21–24, 2018, Copenhagen, Denmark. This paper was recommended for publication in revised form by Associate Editor Gang Tao under the direction of Editor Miroslav Krstic.

* Corresponding author.
E-mail addresses: shahabaldin@bilkent.edu.tr (S.S. Tohidi), yyildiz@bilkent.edu.tr (Y. Yildiz), ilya@umich.edu (I. Kolmanovsky).

https://doi.org/10.1016/j.automatica.2020.109161
0005-1098/

For instance, it is used in Tjønnås and Johansen (2010) to improve the steering performance in faulty automotive vehicles. In another study (Podder & Sarkar, 2001), control allocation distributes propulsive forces of an autonomous underwater vehicle among redundant thrusters so that faults are accommodated. In Sadeghzadeh et al. (2012), experimental results of employing control allocation for quadrotor helicopter are reported. In several applications, fault detection and isolation methods are employed in parallel with control allocation (Ducard, 2009). In Alwi and Edwards (2008), a sliding mode controller is coupled with a pseudo inverse based control allocation to obtain a fault tolerant controller wherein faults are assumed to be estimated. Similarly in Sørensen et al. (2017), it is assumed that there exists a fault detection and isolation scheme which is able to estimate and identify stuck-in-place, hard-over, loss of effectiveness and floating actuator faults. In Cristofaro and Johansen (2014), an unknown input observer is applied to identify actuator and effector faults. A family of unknown input observers is proposed in Cristofaro, Polycarpou, and Johansen (2015) to detect and isolate faults in systems with redundant actuators. In Casavola and Garone (2010) and Tohidi, Khaki et al. (2016), faults are estimated adaptively using recursive least squares, and an online dither generation method is proposed to guarantee the persistence of excitation.

In this paper we consider the following problem: Allocate a control input vector v among redundant constrained actuators in the presence of actuator effectiveness uncertainty. To solve this problem, two subproblems need to be addressed:

(i) Actuator uncertainty: Determine u such that $B\Lambda u+\bar{d}=v$, where Λ represents uncertainty and $\bar{d}$ represents an unknown bounded disturbance. In this paper, we address this problem by proposing an adaptive control allocation method which does not need uncertainty estimation unlike prior approaches.

(ii) Actuator constraints: Determine u such that $B\Lambda u+\bar{d}=v$, where the elements of the actuator signal vector, u, are constrained. One approach to prevent actuators from getting saturated is to determine a set for the control input vector elements, $v_i, i=1,\ldots,r$, and confine them to this set (Corradini, Cristofaro, & Orlando, 2010; Naderi, Sedigh, & Johansen, 2019; Tarbouriech, Garcia, da Silva Jr, & Queinnec, 2011). However, when an adaptive approach is utilized to solve (i), restricting control signals in an attainable set may not prevent actuator saturation. Hence, in addition to restricting control signals to an attainable set, an element-wise non-symmetric projection algorithm is employed in this paper to constrain adaptive parameters.

Other adaptive approaches to control allocation have been described in Falconí and Holzapfel (2016) and Tjønnås and Johansen (2008). As compared to these references, the approach in this paper eliminates the need for uncertainty estimation and persistence of excitation assumption. Furthermore, in the proposed approach, a closed loop reference model (Gibson, Qu, Annaswamy, & Lavretsky, 2015) is employed to achieve fast convergence without inducing undesired oscillations. Apart from these contributions, we also show that it is possible to employ the projection algorithm (Lavretsky & Gibson, 2011) in a stable manner even if the ideal adaptive parameters are not inside the projection boundaries. To the best of our knowledge, such a result is not available in the prior literature.

Preliminary results were reported in our conference papers (Tohidi, Yildiz et al., 2016; Tohidi et al., 2017, 2018). This paper contains additional details and proofs not reported in earlier publications and provides a procedure to account for the actuator saturation in a way that facilitates the design and integration of the controller.

This paper is organized as follows: Section 2 introduces notations and preliminary results. Section 3 presents the uncertain over-actuated plant dynamics and the proposed model reference adaptive control allocation approach with a closed loop reference model. A discussion of actuator saturation and its effects on the control limits together with the projection algorithm are given in Section 4. The ADMIRE model is used in Section 5 to demonstrate the effectiveness of the proposed approach in the simulation environment. Finally, a summary is given in Section 6.

2. Notations and preliminaries

In this section, we collect several definitions and basic results which are exploited in the following sections. Throughout this paper, $\|.\|$ refers to the Euclidean norm for vectors and induced 2-norm for matrices, and $\|.\|_F$ refers to the Frobenius norm. $\lambda_{min}(.)$, $\lambda_{max}(.)$ and $\lambda_i(.)$ refer to the minimum, maximum and ith eigenvalue of a matrix, respectively. Also, $\text{row}_i(.)$ and $\text{column}_i(.)$ refer to the ith row and column of a matrix, respectively, and $\text{vec}(.):\mathbb{R}^{r\times m}\to\mathbb{R}^{rm}$ puts the elements of a matrix in a column vector. I_r is an identity matrix of dimension $r\times r$ and $tr(.)$ refers to the trace operation.

The element-wise projection $\text{Proj}(\theta_{v_{i,j}}, Y_{i,j}, f):\mathbb{R}\times\mathbb{R}\times\mathcal{F}\to\mathbb{R}$ is defined as

$$\text{Proj}(\theta_{v_{i,j}}, Y_{i,j}, f) \equiv \begin{cases} Y_{i,j} - Y_{i,j} f(\theta_{v_{i,j}}) & \text{if } f(\theta_{v_{i,j}})>0 \ \&\ Y_{i,j}(\frac{df}{d\theta_{v_{i,j}}})>0 \\ Y_{i,j} & \text{otherwise,} \end{cases} \tag{1}$$

where $f(.)\in\mathcal{F}(\mathbb{R}\to\mathbb{R})$ is a convex and continuously differentiable (C^1) function defined as

$$f(\theta_{v_{i,j}}) = \frac{(\theta_{v_{i,j}} - \theta_{min_{i,j}} - \zeta_{i,j})(\theta_{v_{i,j}} - \theta_{max_{i,j}} + \zeta_{i,j})}{(\theta_{max_{i,j}} - \theta_{min_{i,j}} - \zeta_{i,j})\zeta_{i,j}}, \tag{2}$$

and where $\zeta_{i,j}$ is the projection tolerance of the (i,j)th element of θ_v that should be chosen as $0<\zeta_{i,j}<0.5(\theta_{max_{i,j}}-\theta_{min_{i,j}})$. $\theta_{max_{i,j}}$ and $\theta_{min_{i,j}}$ are the upper and lower bounds of the (i,j)th element of θ_v. These bounds also form the projection set, $\Omega_{\text{proj}} = \{\theta_v : \theta_{v_{i,j}}\in[\theta_{min_{i,j}},\ \theta_{max_{i,j}}]\}$. A useful subset of Ω_{proj} is defined as $\hat{\Omega}_{\text{proj}} = \{\theta_v : \theta_{v_{i,j}}\in[\theta_{min_{i,j}}+\zeta_{i,j},\ \theta_{max_{i,j}}-\zeta_{i,j}]\}$. For $\theta_v\in\Omega_{\text{proj}}$ and $\theta_v^*\in\hat{\Omega}_{\text{proj}}$, the following inequality holds (Lavretsky & Gibson, 2011):

$$tr((\theta_v^T - \theta_v^{*T})(-Y + \text{Proj}(\theta_v, Y, f))) \le 0, \tag{3}$$

where $\theta_v\in\Omega_{\text{proj}}\subset\mathbb{R}^{r\times m}$, $Y\in\mathbb{R}^{r\times m}$.

3. Control allocation problem

The closed loop system studied in this paper is presented in Fig. 1. The plant dynamics are given by

$$\dot{x}(t) \quad = Ax(t) + B_u(\Lambda u(t) + d_u(t)), \tag{4}$$

where $x\in\mathbb{R}^n$ is the state vector, $u=[u_1,\ldots,u_m]^T\in\mathbb{R}^m$ is the actuator input vector, $A\in\mathbb{R}^{n\times n}$ and $B_u\in\mathbb{R}^{n\times m}$ are known matrices and $d_u\in\mathbb{R}^m$ is a bounded disturbance input. The matrix $\Lambda\in\mathbb{R}^{m\times m}$ is assumed to be diagonal, with positive elements representing actuator effectiveness uncertainty. It is assumed that the pair $(A, B_u\Lambda)$ is controllable. Due to actuator redundancy, the input matrix is rank deficient, that is $\text{Rank}(B_u)=r<m$. Consequently, B_u can be written as $B_u=B_vB$, where $B_v\in\mathbb{R}^{n\times r}$ is a full column rank matrix, and $B\in\mathbb{R}^{r\times m}$ is a full row rank matrix. This decomposition of B_u helps exploit the actuator redundancy using control allocation. Employing this decomposition, (4) can be rewritten as

$$\dot{x}(t) = Ax(t) + B_v(B\Lambda u(t) + \bar{d}(t)), \tag{5}$$

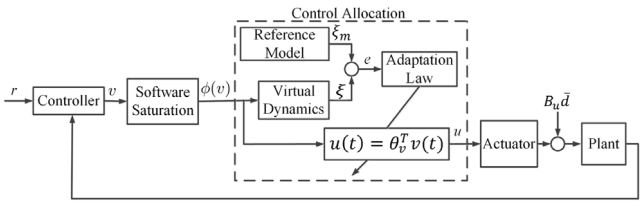

Fig. 1. Block diagram of the closed loop system with the proposed control allocation method.

where $\bar{d}(t) = Bd_u(t)$ is assumed to have an upper bound. The actuator range limits are $u_i \in [-u_{\max_i}, u_{\max_i}], u_{\max_i} > 0, i = 1, \ldots, m$. The actuator saturation will be addressed both in the design of our adaptive control allocation and by passing the output of the controller, v, through a software saturation function, $\phi(\cdot) : \mathbb{R}^r \to \mathbb{R}^r$ in Fig. 1, the requirement for latter will be discussed in Section 4. The adaptive control allocation task is to achieve

$$B\Lambda u(t) + \bar{d}(t) = \phi(v(t)), \tag{6}$$

which would lead to

$$\dot{x}(t) = Ax(t) + B_v\phi(v(t)). \tag{7}$$

Remark 1. The focus of this paper is not the adaptive control of the plant (4), for which various solutions exist (Narendra & Annaswamy, 2012; Tao, 2003) but the control allocation problem of achieving (6) when Λ is unknown and there are actuator limits. Our objective is to characterize the mismatch between $\phi(v(t))$ and $B\Lambda u(t)+\bar{d}(t)$ due to transients in control allocation dynamics so that it can be accounted for in the design of the controller which generates the signal v. In typical applications, such as flight control, the controller may not be adaptive. Hence, it is desirable to handle actuator uncertainty within the control allocation layer.

Remark 2. The treatment of nonlinear time-varying uncertainties represents a direction for future work.

In order to achieve (6), the following virtual dynamics,

$$\dot{\xi}(t) = A_m\xi(t) + B\Lambda u(t) + \bar{d}(t) - \phi(v(t)), \tag{8}$$

where $A_m \in \mathbb{R}^{r\times r}$ is a stable matrix, and the reference model

$$\dot{\xi}_m(t) = A_m\xi_m(t), \tag{9}$$

is constructed. Defining the actuator input as a mapping from v to u,

$$u(t) = \theta_v^T(t)\phi(v(t)), \tag{10}$$

where $\theta_v \in \mathbb{R}^{r\times m}$ represents the adaptive parameter matrix to be determined, and substituting (10) into (8), we obtain

$$\dot{\xi}(t) = A_m\xi(t) + (B\Lambda\theta_v^T(t) - I_r)\phi(v(t)) + \bar{d}(t). \tag{11}$$

Let $\theta_v^* \in \mathbb{R}^{r\times m}$ be the ideal θ_v matrix, such that

$$B\Lambda\theta_v^{*T} = I_r, \tag{12}$$

and note that under our assumptions such θ_v^* always exists. Defining $e = \xi - \xi_m$ and subtracting (9) from (11), it follows that

$$\dot{e}(t) = A_m e(t) + B\Lambda\tilde{\theta}_v^T(t)\phi(v(t)) + \bar{d}(t), \tag{13}$$

where $\tilde{\theta}_v(t) = \theta_v(t) - \theta_v^*$.

Theorem 1. *Consider (8) and (9), and assume that there exists a positive scalar D such that $\|\bar{d}(t)\| \le D$ for all $t \ge 0$. Suppose that the adaptive parameter matrix is updated using the following adaptive law,*

$$\dot{\theta}_v(t) = \Gamma_\theta Proj\big(\theta_v(t), -\phi(v(t))e^T(t)PB, f\big), \tag{14}$$

where the symmetric positive definite matrix P satisfies $A_m^TP + PA_m = -Q$, Q is a symmetric positive definite matrix, the projection operator "Proj" is defined in (1), with convex function $f \in C^1$ in (2), and $\Gamma_\theta = \gamma_\theta I_r$, $\gamma_\theta > 0$. Then given any initial condition $e(0) \in \mathbb{R}^r$, $\theta_v(0) \in \Omega_{proj}$, and $\theta_v^* \in \hat{\Omega}_{proj}$, $e(t)$ and $\tilde{\theta}_v(t)$ remain uniformly bounded for all $t \ge 0$ and their trajectories converge exponentially to the set

$$E_1 = \{(e, \tilde{\theta}_v) : \|e\|^2 \le \Big(\frac{s\tilde{\theta}_{max}^2}{\gamma_\theta\lambda_{min}(Q)} + \frac{2\chi^4D^2\|Q\|^2}{\sigma^2\lambda_{min}(Q)^2}\Big) \times \frac{4s\chi^2\|Q\|}{\sigma\lambda_{min}(Q)}, \|\tilde{\theta}_v\| \le \tilde{\theta}_{max}\}, \tag{15}$$

where $s = -\min_i(\lambda_i(A_m + A_m^T)/2)$, $\sigma = -\max_i(Real(\lambda_i(A_m)))$, $\chi = \frac{3}{2}(1 + 4\frac{a}{\sigma})^{(r-1)}$, $a = \|A_m\|$ and $\|\tilde{\theta}_v(t)\|_F \le \tilde{\theta}_{max} \equiv \sqrt{\sum_{i,j}(\theta_{max_{i,j}} - \theta_{min_{i,j}} - \zeta_{i,j})^2}$. In addition, if $\bar{d}(t) = 0$ for $t \ge t'$ for some $t' \ge 0$ and $\phi(v(t))$ is uniformly continuous as a function of $t \in [t', +\infty)$, then $B\Lambda u(t) \to \phi(v(t))$ as $t \to \infty$, i.e., (6) is achieved asymptotically.

Proof. See Appendix A. □

Theorem 1 implies that θ_v and e are bounded. Considering that $\phi(v)$ is bounded, (10) implies that u is bounded. Since A_m is Hurwitz, the variable ξ, whose dynamics is given in (8), is also bounded. Therefore, all the signals in the adaptive control allocation system are bounded.

Remark 3. To realize (8), the signal $B\Lambda u + \bar{d}$, is required. In motion control applications, this signal corresponds to the net forces and moments (see Härkegård, 2003, for example, for an aerospace application), that can be obtained via an inertial measurement unit (IMU). Examples of measuring/estimating this signal, without introducing delay or noise amplification, and employing it in real applications can be found in Kutay et al. (2007) and Sieberling, Chu, and Mulder (2010).

Remark 4. A sufficient but not necessary condition for the uniform continuity of $\phi(v(t))$ is that its time rate of change is bounded, which can be ensured, e.g., by extending the software saturation function to include the rate limiting. (see Fig. 1).

Remark 5. The proposed control allocation method uses the signal $\phi(v(t))$, which is the output of the software saturation. The saturation limits are determined based on the attainable set for v, the details of which are given in Section 4. The control allocator then determines the actuator signals, $u_i, i = 1, 2, \ldots, m$, that do not saturate the actuators. Note that putting a bound on v using soft saturation does not necessarily imply that the actuators will not be saturated by u_i. To prevent actuator saturation, the boundaries of the projection operator in (14) must be selected carefully, as further detailed in Section 4.

Remark 6. In the case the assumption $d(t) = 0$, for $t \ge t'$ for some $t' \ge 0$ is not made, a bound similar to E_1 can be derived for the control allocation error, $B\Lambda u + \bar{d} - \phi(v)$. However, note that even though only a boundedness result can be given for the control allocation error, the tracking error for the overall closed loop system can still be forced to converge to zero by an appropriately designed controller (see Remark 11).

Remark 7. $\theta_v^* \in \mathbb{R}^{r\times m}$ is the ideal parameter matrix that should satisfy (12). Since Λ is unknown, θ_v^* is also unknown. However, although the diagonal matrix Λ is unknown, its elements are in the interval $(0,\ 1]$. Thus, using (12), the set Ω^* that contains all possible values of θ_v^* can be defined.

Conventionally, it is assumed that the projection boundaries, $\theta_{min_{i,j}}$ and $\theta_{max_{i,j}}$, are chosen such that $\theta_v^* \in \Omega^* \subset \hat{\Omega}_{\text{proj}} \subset \Omega_{\text{proj}}$. However, such a choice may not be consistent with the actuator limits as further discussed in Section 4.

Remark 8. Let $\theta_v^* \in \Omega^*$, $\Omega^* \not\subset \hat{\Omega}_{\text{proj}}$ and consider the projection algorithm (1) with convex function (2). Then, $\tilde{\theta}_{max}$, defined in Theorem 1, should be redefined as

$$\tilde{\theta}_{MAX} \equiv \sqrt{\sum_{i,j}(\max(|\theta^*_{max_{i,j}} - \theta_{min_{i,j}} - \zeta_{i,j}|, |\theta^*_{min_{i,j}} - \theta_{max_{i,j}} + \zeta_{i,j}|))^2}. \tag{16}$$

We note that to differentiate two different cases (the ideal parameter θ_v^* being inside or outside the projection bounds), the maximum value of adaptive parameter deviation from its ideal value is designated by $\tilde{\theta}_{max}$ for the former and $\tilde{\theta}_{MAX}$ for the latter case. Below, we provide a lemma and a theorem, regarding the stability of the control allocation for the latter case, i.e. when $\theta_v^* \notin \hat{\Omega}_{\text{proj}}$.

Lemma 1. *For $\theta_v^* \notin \hat{\Omega}_{proj}$, $\theta_{v_{i,j}} \in \mathbb{R}^{r\times m}$, $Y \in \mathbb{R}^{r\times m}$ with $r \le m$ and the projection algorithm (1)–(2), the following inequality holds:*

$$tr((\theta_v^T - \theta_v^{*T})(-Y + Proj(\theta_v, Y))) \le \sqrt{r}\tilde{\theta}_{MAX}\|Y\|. \tag{17}$$

Proof. See Appendix B. □

Theorem 2. *Consider (8), (9), (10), and (14). Assume that there exist positive scalars M and D such that $\|\phi(v(t))\| \le M$ and $\|\bar{d}(t)\| \le D$ for all $t \ge 0$. Then, for any initial condition $e(0) \in \mathbb{R}^r$, $\theta_v(0) \in \Omega_{proj}$, and $\theta_v^* \notin \hat{\Omega}_{proj}$, $e(t)$ and $\tilde{\theta}_v(t)$ are uniformly bounded for all $t \ge 0$ and their trajectories converge exponentially to the closed and bounded set*

$$\hat{E}_1 = \{(e,\tilde{\theta}_v) : \|\tilde{\theta}_v\| \le \tilde{\theta}_{MAX},\ \|e\|^2 \le (\frac{s\tilde{\theta}^2_{MAX}}{\gamma_\theta \lambda_{min}(Q)} + \frac{4\chi^4\|Q\|^2(D^2 + r\tilde{\theta}^2_{MAX}\|B\|^2M^2)}{\sigma^2\lambda_{min}(Q)^2})\frac{4s\chi^2\|Q\|}{\sigma\lambda_{min}(Q)}\}, \tag{18}$$

where $s = -\min_i(\lambda_i(A_m + A_m^T)/2)$, $\sigma = -\max_i(Real(\lambda_i(A_m)))$, $\chi = \frac{3}{2}(1 + 4\frac{a}{\sigma})^{(r-1)}$, $a = \|A_m\|$ and $\tilde{\theta}_{MAX}$ is defined in (16).

Proof. See Appendix C. □

To obtain fast convergence without introducing excessive oscillations, (9) is modified to obtain the following closed loop reference model (Gibson et al., 2015)

$$\dot{\xi}_m(t) = A_m\xi_m(t) - L(\xi(t) - \xi_m(t)), \tag{19}$$

where $A_m \in \mathbb{R}^{r\times r}$ is Hurwitz, $L = -\ell I_r$, $\ell > 0$. Defining $\bar{A}_m = A_m + L$, and subtracting (19) from (11), we get

$$\dot{e}(t) = \bar{A}_m e(t) + B\Lambda\tilde{\theta}_v^T(t)\phi(v(t)) + \bar{d}(t). \tag{20}$$

We assume that the matrix $\bar{A}_m$ is Hurwitz through an appropriate selection of L.

Theorem 3. *Consider (8), the reference model (19), the actuator signal (10), and the adaptive law*

$$\dot{\theta}_v(t) = \Gamma_\theta Proj(\theta_v(t), -\phi(v(t))e(t)^T\bar{P}B, f), \tag{21}$$

where the symmetric positive definite matrix $\bar{P}$ satisfies $\bar{A}_m^T\bar{P} + \bar{P}\bar{A}_m = -\bar{Q}$, $\bar{Q}$ is a symmetric positive definite matrix, $\Gamma_\theta^{-1} = (1/\gamma_\theta)I_r$, $\gamma_\theta > 0$ and the projection is defined by (1) and (2). Assume that there exist positive scalars M and D such that $\|\phi(v(t))\| \le M$ and $\|\bar{d}(t)\| \le D$ for all $t \ge 0$. Then, for any initial condition $e(0) \in \mathbb{R}^r$, and $\theta_v(0) \in \Omega_{proj}$, $e(t)$ and $\tilde{\theta}(t)$ are uniformly bounded for all $t \ge 0$ and their trajectories converge exponentially to a closed and bounded set

$$E_2 = \{(e,\tilde{\theta}_v) : \|e\|^2 \le (\frac{(s+\ell)\tilde{\theta}^2_{max}}{\gamma_\theta\lambda_{min}(Q)} + \frac{2\bar{\chi}^4D^2\|Q\|^2}{\bar{\sigma}^2\lambda_{min}(Q)^2}) \times \frac{4(s+\ell)\bar{\chi}^2\|Q\|}{\bar{\sigma}\lambda_{min}(Q)},\ \|\tilde{\theta}_v\| \le \tilde{\theta}_{max}\},$$

if $\theta^*_{v_{i,j}} \in \hat{\Omega}_{proj}$, or to closed and bounded set

$$\hat{E}_2 = \{(e,\tilde{\theta}_v) : \|\tilde{\theta}_v\| \le \tilde{\theta}_{MAX},\ \|e\|^2 \le (\frac{(s+\ell)\tilde{\theta}^2_{MAX}}{\gamma_\theta\lambda_{min}(Q)} + \frac{4\bar{\chi}^4\|Q\|^2(D^2 + r\tilde{\theta}^2_{MAX}\|B\|^2M^2)}{\bar{\sigma}^2\lambda_{min}(Q)^2})\frac{4(s+\ell)\bar{\chi}^2\|Q\|}{\bar{\sigma}\lambda_{min}(Q)}\},$$

if $\theta^*_{v_{i,j}} \notin \hat{\Omega}_{proj}$, where $\bar{\sigma} = -\max_i(Real(\lambda_i(\bar{A}_m)))$, $s = -\min_i(\lambda_i(A_m + A_m^T)/2)$, $\bar{a} = \|\bar{A}_m\|$ and $\bar{\chi} = \frac{3}{2}(1 + 4\frac{\bar{a}}{\bar{\sigma}})^{(r-1)}$.

Proof. The proof procedure is similar to the one for Theorems 1 and 2, and is omitted for brevity. □

4. Determination of the projection set

In the previous section, the control allocator was designed based on the projection operator. In this section, the determination of the projection set, Ω_{proj}, which defines the bounds on adaptive control parameters, is detailed. The projection set is determined to satisfy two requirements: (1) The actuator command signals, $u_i, i = 1, \ldots, m$, should not saturate the actuators and (2) a specific condition (to be introduced shortly) which is necessary for the controller and control allocation integration, should be satisfied. The design procedure to achieve these goals is composed of three main steps. First, an attainable set for control signal vector v is found for $\Lambda = I_m$, which is used to determine the software saturation function $\phi(.)$. Secondly, a compact set for the adaptive parameter θ_v is calculated, to satisfy $-u_{max} \le \theta_v^T\phi(v) \le u_{max}$. Thirdly, the projection set that satisfies the specific requirement necessary for the controller and control allocation integration is determined.

Step 1: Realizable values of control signals are found.

The actuator constraints are known: $u(t) \in \Omega_u$, where $\Omega_u = \{[u_1, \ldots, u_m]^T : -u_{max_i} \le u_i \le u_{max_i}, i = 1, \ldots, m\}$, $u_{max_i} > 0, i = 1, \ldots, m$. Using Ω_u, the set Ω_v, defining all realizable values of the control input v, can be obtained as $\Omega_v = \{v : v = Bu, u \in \Omega_u, B^\dagger v \in \Omega_u\}$, where $(.)^\dagger$ refers to the pseudo inverse of a non-square matrix. Furthermore, there exist $M_i, i = 1, \ldots, r$, such that $\hat{\Omega}_v \equiv \{v : v_i \in [-M_i, M_i], i = 1, \ldots, r\} \subset \Omega_v$. The set $\hat{\Omega}_v$ can be used to define the constraints which are enforced using a software saturation function, whose output is $\phi(v(t))$. See Fig. 1 and Remark 5.

Step 2: The boundaries for the adaptive parameters to ensure that the actuator signal vector u does not saturate the actuators are calculated.

A subset of the attainable set for the control signals, $\hat{\Omega}_v$, was obtained in Step 1. The actuator limits are known. With this information, the set $\Omega_\theta = \{\theta_v : -u_{max} \le \theta_v^T\phi(v) \le u_{max}, \phi(v) \in \hat{\Omega}_v\}$ can be obtained. Let $\theta_I^* = B^\dagger$ which corresponds to an adaptive parameter value in the absence of uncertainty, i.e., $\Lambda = I$. Since $\phi(v) \in \hat{\Omega}_v \subset \Omega_v$, we have $B^\dagger\phi(v) = \theta_I^{*T}\phi(v) \in \Omega_u$, for all

$\phi(v) \in \hat{\Omega}_v$. Therefore, $\theta_l^* \in \Omega_\theta$, which is required to subsequently solve the optimization problem (25) (see Remark 9).

Step 3: A subset of Ω_θ, which satisfies a necessary condition for a stabilizing controller, is obtained. This subset of Ω_θ also determines the ultimate projection boundaries, and is denoted by Ω_{proj}.

The plant dynamics (5), can be rewritten, by using (10), (12) and defining $\tilde{\theta}_v = \theta_v - \theta_v^*$, as

$$\begin{aligned}\dot{x} &= Ax + B_v(B\Lambda u + \bar{d}) = Ax + B_v(B\Lambda\theta_v^T\phi(v) + \bar{d})\\ &= Ax + B_v(I + B\Lambda\tilde{\theta}_v^T)\phi(v) + B_v\bar{d},\end{aligned} \tag{22}$$

where $\phi(v) \in \hat{\Omega}_v$ and $\bar{d}$ is a bounded disturbance. Note that the projection algorithm guarantees that the actuators do not saturate, and the closed loop system does not see any residual disturbance due to saturation of the actuators. Defining $\Delta B(t) \equiv B\Lambda\tilde{\theta}_v^T(t)$, and substituting in (22), it follows that

$$\dot{x}(t) = Ax(t) + B_v(\phi(v(t)) + d(t)), \tag{23}$$

where $d(t) = \Delta B(t)\phi(v(t)) + \bar{d}(t) \in \mathbb{R}^r$.

To be able to design a stabilizing controller, which will produce the control input v, one must make sure that each element of the disturbance vector $d = [d_1, \ldots, d_r]^T$ in (23), is smaller in absolute value than the upper bound of the corresponding element of the saturated control input, $\phi(v)$, that is $|d_i| < M_j$, $i = 1, \ldots, r$. Since $d_i = \text{row}_i(\Delta B)v + \bar{d}_i$, $i = 1, \ldots, r$, where $\bar{d}_i$ is the ith element of $\bar{d}$, satisfying the following condition ensures that $|d_i| < M_i$, $i = 1, \ldots, r$:

$$M_i - \|\text{row}_i(\Delta B)\|M_{\max} > |\bar{d}_i|, \;\; i = 1, \ldots, r, \tag{24}$$

where $M_{\max} = \max_i M_i$. A necessary condition for satisfying the inequality (24) is $\|\text{row}_i(\Delta B)\| = \|\text{row}_i(B\Lambda\tilde{\theta}_v^T)\| < M_i/M_{\max}$ for all $i = 1, \ldots, r$. (Sufficient conditions required to satisfy (24) are discussed later in Remark 10.) Thus, the elements of the matrix θ_v should be properly bounded in order to satisfy the necessary condition $\|\text{row}_i(B\Lambda\tilde{\theta}_v^T)\| < M_i/M_{\max}$ for all $i = 1, \ldots, r$, and for all $\Lambda \in \hat{\Omega}_\Lambda$, where $\hat{\Omega}_\Lambda \subset \Omega_\Lambda$, and Ω_Λ is the set of all $m \times m$ diagonal matrices with elements in $(0, 1]$. Thus $\hat{\Omega}_\Lambda$ has diagonal elements $\lambda_i \in (\gamma, 1]$, where γ is precisely defined later in Theorem 4.

Since $B\Lambda\tilde{\theta}_v^T = B\Lambda(\theta_v^T - \theta_v^{*T}) = B\Lambda\theta_v^T - I_r$, the solution, R, of the optimization problem,

$$\begin{aligned}R^2 = &\min_{\theta_v} \left(\text{vec}(\theta_v - \theta_l^*)^T\text{vec}(\theta_v - \theta_l^*)\right) \\ s.t. \;\; &\left\|\text{row}_i(B\Lambda\theta_v^T - I_r)\right\|^2 = \frac{M_i^2}{M_{\max}^2} - \epsilon, \quad i = 1, \ldots, r,\\ &\Lambda \in \hat{\Omega}_\Lambda, \quad \theta_v \in \Omega_\theta,\end{aligned} \tag{25}$$

which is solved offline, is the minimum distance from the $\text{vec}(\theta_l^*)$ to the boundary of the set

$$\begin{aligned}\Psi = \{&\theta_v : \|\text{row}_i(B\Lambda\theta_v^T - I_r)\|^2 \le \frac{M_i^2}{M_{\max}^2} - \epsilon,\\ &\Lambda \in \hat{\Omega}_\Lambda, \theta_v \in \Omega_\theta, i = 1, \ldots, r\},\end{aligned} \tag{26}$$

where ϵ is a small positive constant used to have a closed set, since typical numerical optimizers optimize only over a closed set. It is noted that the corresponding $\theta_{max_{i,j}}$ and $\theta_{min_{i,j}}$ are not unique, and different boundaries can be found by defining different cost functions in (25). With the calculated $\theta_{max_{i,j}}$ and $\theta_{min_{i,j}}$, the projection set is obtained as,

$$\Omega_{\text{proj}} = \{\theta_v : \theta_{i,j} \in [\theta_{min_{i,j}}, \;\; \theta_{max_{i,j}}]\}. \tag{27}$$

Remark 9. For all elements of $\hat{\Omega}_\Lambda$, the optimization problem (25) finds the largest neighborhood of θ_l^* in Ω_θ that satisfies $\|\text{row}_i(\Delta B)\| < M_i/M_{\max}$, $i = 1, \ldots, r$. This neighborhood is an n-sphere, with the center at $\text{vec}(\theta_l^*)$ and with the radius R.

To show that the optimization problem (25) is feasible, it should be proven that the set Ψ always includes $\text{vec}(\theta_l^*)$.

Theorem 4. *The set* $\Upsilon = \{vec(\theta_v) : \|row_i(B\Lambda\theta_v^T - I_r)\|^2 \le \frac{M_i^2}{M_{max}^2} - \epsilon, \Lambda \in \hat{\Omega}_\Lambda \subset \Omega_\Lambda, i = 1, \ldots, r\} \cap vec(\theta_l^*) \neq \varnothing$ *when* $\lambda_{min}(\Lambda) \ge \gamma \equiv \max_i(1 - \sqrt{\gamma_{M_i}/\gamma_{B_i}})$, *where* $\gamma_{B_i} \equiv \|row_i(B)\|\|B^T(BB^T)^{-1}\|$ *and* $\gamma_{M_i} \equiv \frac{M_i^2}{M_{max}^2} - \epsilon$.

Proof. See Appendix D. □

Based on the definition of γ_{B_i}, γ_{M_i} and γ given in Theorem 4, $\hat{\Omega}_\Lambda$ is defined as

$$\hat{\Omega}_\Lambda = \{\Lambda : \Lambda \in \mathbb{D}^{m\times m}, \;\; \text{diag}_i(\Lambda) \in (\gamma, 1], \;\; i = 1, \ldots, m\}, \tag{28}$$

where $\mathbb{D}$ denotes the set of real diagonal matrices, and $\text{diag}_i(.) : \mathbb{R}^{m\times m} \to \mathbb{R}$ provides the ith diagonal element of square matrices.

Remark 10. Using $\hat{\Omega}_\Lambda$, defined in (28), and Ω_{proj}, defined in (27), the upper bound on $\|\text{row}_i(\Delta B)\| = \|\text{row}_i(B\Lambda\tilde{\theta}_v^T)\|$ can be found, which we denote as ρ_i, $i = 1, \ldots, r$. Therefore, recalling that M_i is defined as the upper bound on the absolute value of ith control signal v_i, and considering (24), $|\bar{d}_i|$ should be smaller than $M_i - \rho_i M_{\max}$, i.e. $|\bar{d}_i| < M_i - \rho_i M_{\max}$. Note that $\rho_i < \frac{M_i}{M_{\max}}$ is guaranteed by the solution of (25). Therefore, the condition $|d_i| < M_i$ is satisfied.

Remark 11. A step by step procedure for the control allocation design is provided in Appendix E. Note that in the presence of the control allocator, the system dynamics takes the form of (23). The controller, which will produce the control signal v, needs to be designed in the presence of the saturation nonlinearity represented by $\phi(.)$ and the bounded disturbance d. Tracking controllers for (23) can be designed using, for instance, the methods presented in Corradini et al. (2010). See also Tohidi, Yildiz et al. (2016), Tohidi et al. (2017) which illustrate the process of integrating an initial version of our control allocation scheme and a controller. We omit details for lack of space.

5. Simulation results

The Aerodata Model in Research Environment (ADMIRE), which represents the dynamics of an over-actuated aircraft model, is used to demonstrate the effectiveness of the adaptive control allocation in the presence of uncertainty and actuator constraints. The linearized ADMIRE model (Härkegård & Glad, 2005) is given below:

$$\begin{aligned}&\dot{x} = Ax + B_u u = Ax + B_v v,\\ &v = Bu, \quad B_u = B_v B, \quad B_v = [0_{3\times 2} \; I_{3\times 3}]^T,\end{aligned} \tag{29}$$

where $x = [\alpha \;\; \beta \;\; p \;\; q \;\; r]^T$ with α, β, p, q and r denote the angle of attack, sideslip angle, roll rate, pitch rate and yaw rate, respectively. The vector $u = [u_c \; u_{re} \; u_{le} \; u_r]^T$ represents the control surface deflections of canard wings, right and left elevons and the rudder. The position limits of the control surfaces are given as $u_c \in [-55, 25] \times \frac{\pi}{180}$ rad, $u_{re}, u_{le}, u_r \in [-30, 30] \times \frac{\pi}{180}$ rad and the actuators have first-order dynamics and a time constant of 0.05 s. The state and control matrices are given in Härkegård and Glad (2005). To represent actuator loss of effectiveness and disturbance, a diagonal matrix Λ and a vector d_u, respectively, are augmented to the model (29) as

$$\begin{aligned}&\dot{x} = Ax + B_u\Lambda u + B_u d_u = Ax + B_v v + B_v\bar{d}\\ &v = B\Lambda u, \quad \bar{d} = Bd_u, \quad B_u = B_v B, \quad B_v = [0_{3\times 2} \; I_{3\times 3}]^T.\end{aligned} \tag{30}$$

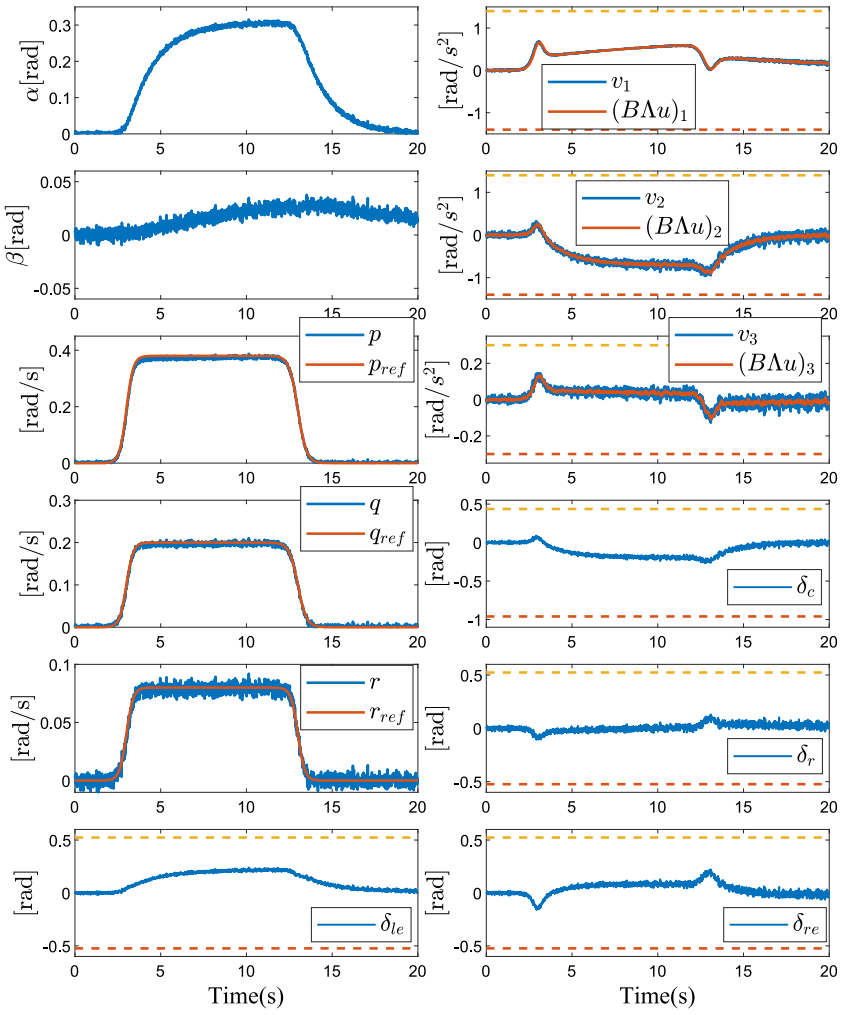

Fig. 2. System states, control signals and actuators' deflections using conventional control allocation when actuator loss of effectiveness is $\Lambda_1 = I$.

In the simulations, the disturbance $\bar{d}$ is a sinusoidal function with amplitude 0.1 and frequency 1 rad/s while zero-mean white Gaussian noise with standard deviation $\sigma_{p,q,r} = 0.0017$ rad/s for the angular rates and $\sigma_{\alpha,\beta} = 0.0044$ rad for angles represent the measurement noise (Sieberling et al., 2010). For all of the simulations a sliding mode controller is used to create the control signal v. The simulation results for a conventional pseudo inverse based control allocation are reported in Fig. 2 for the case without actuator loss of effectiveness, that is, $\Lambda_1 = I$. With the actuator loss of effectiveness modeled as changing the diagonal elements of Λ from 1 to 0.85 at $t = 7$ s, the simulation results for the conventional control allocation are given in Fig. 3. It is seen that 15% loss of effectiveness in all actuators at $t = 7$ s causes instability. The proposed adaptive control allocation introduced in Section 3 is used in the simulations. Using Steps 1–3 in Section 4, the values of $M_1 = 1.4$, $M_2 = 1.4$ and $M_3 = 0.3$ are obtained and Ω_{proj}, which determines the maximum and minimum of each element of the adaptive parameter matrix is computed corresponding to $\theta_{v_{1,1}} \in [-0.0129, 0.0129]$, $\theta_{v_{1,2}} \in [0.0307, 0.5225]$, $\theta_{v_{1,3}} \in [-0.1357, 0.1371]$, $\theta_{v_{1,4}} \in [-0.212, 0]$, $\theta_{v_{2,1}} \in [-0.3149, -0.1113]$, $\theta_{v_{2,2}} \in [-0.217, -0.1416]$, $\theta_{v_{2,3}} \in [-0.0241, 0.2363]$, $\theta_{v_{2,4}} \in [-0.4162, -0.01]$, $\theta_{v_{3,1}} \in [0.1587, 0.1977]$, $\theta_{v_{3,2}} \in [0.0673, 0.0675]$, $\theta_{v_{3,3}} \in [-0.001, 0.001]$, $\theta_{v_{3,4}} \in [-1.2755, -0.7641]$. We use a closed loop reference model with $l = 4$ and A_m selected as $A_m = diag([-0.2, -0.1, -0.1])$. Fig. 4 shows the simulation results for the system with adaptive control allocation and 15% actuator loss of effectiveness at $t = 7$ s. It is seen that the first two states, α and β, are bounded, and the other states (p, q and r) follow the reference inputs (p_{ref}, q_{ref} and r_{ref}) after the introduction of 15% actuator loss of effectiveness at $t = 7$ sec. Also, it is seen that the elements of $(B\Lambda u)_i$ for $i = 1, 2, 3$, converge to the control signal elements v_i for $i = 1, 2, 3$. Finally, as seen from Figs. 2, 3, and 4, the existence of noise does not affect the adaptive control allocation performance compared to the non-adaptive fixed control allocation. Another scenario is considered next, where the diagonal elements of Λ change from 1 to 0.5 at $t = 7$ s. It is seen in Fig. 5 that the system remains stable even after the introduction of the 50% loss of effectiveness.

6. Summary

An adaptive control allocation for uncertain over-actuated systems with actuator saturation is proposed in this paper. The method needs neither uncertainty identification nor persistence of excitation assumption. Simulation results with the ADMIRE model show the effectiveness of the proposed method.

Appendix A. Proof of Theorem 1

Consider a Lyapunov function candidate,

$$V = e^T P e + tr(\tilde{\theta}_v^T \Gamma_\theta^{-1} \tilde{\theta}_v \Lambda). \tag{A.1}$$

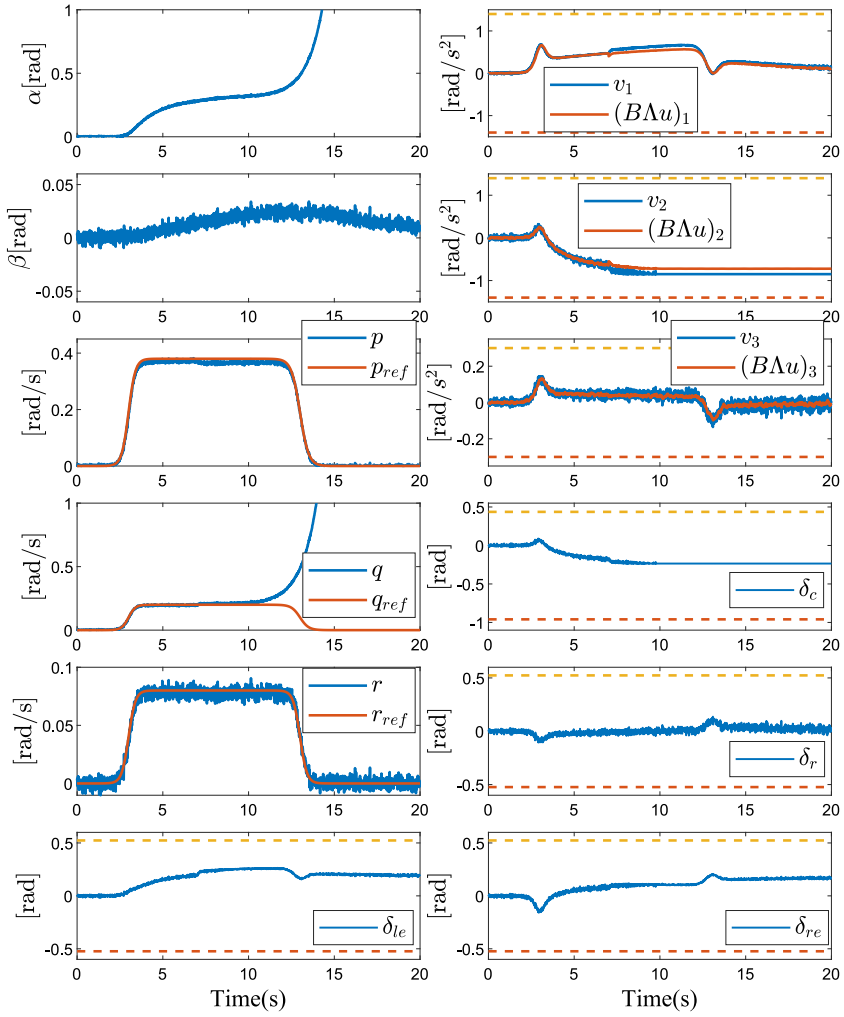

Fig. 3. System states, control signals and actuators' deflections using conventional control allocation when actuator loss of effectiveness is 15% after $t = 7$ s.

The time derivative of (A.1) along the trajectories of (13)–(14) can be calculated as

$$\dot{V} = -e^T Qe + 2e^T PB\Lambda\tilde{\theta}_v^T v + 2tr(\tilde{\theta}_v^T \Gamma_\theta^{-1}\dot{\tilde{\theta}}_v \Lambda) + 2e^T P\bar{d}. \tag{A.2}$$

Using the property of the trace operation and the adaptive law (14), (A.2) can be written as

$$\begin{aligned}\dot{V} &= -e^T Qe + 2e^T P\bar{d} \\ &+ 2tr(\tilde{\theta}_v^T(ve^T PB + \text{Proj}(\theta_v, -ve^T PB, f))\Lambda).\end{aligned} \tag{A.3}$$

If $\bar{d}(t) = 0$ for $t \geq 0$ (without loss of generality), it can be shown, by using (3), that $\dot{V} \leq 0$ and therefore $e(t)$ and $\tilde{\theta}_v(t)$ are bounded. Since $e \in \mathcal{L}_2$ and $\dot{e} \in \mathcal{L}_\infty$, $e(t)$ converges to zero as $t \to \infty$ (Tao, 2003). Since θ_v, e and $\phi(v)$ are bounded, $\dot{\theta}_v$ is also bounded by (14). In addition, since e, $\tilde{\theta}_v$ and v are bounded, $\dot{e}$ is also bounded by (13). Therefore, e and $\tilde{\theta}_v$ are uniformly continuous functions. If v is also uniformly continuous, then $\dot{e}$ is uniformly continuous by (13) since the multiplication of bounded and uniformly continuous functions are uniformly continuous. Then, according to Barbalat's lemma, $\dot{e}(t)$ converges to zero as $t \to \infty$. Since both e and $\dot{e}$ converge to zero, by (13) $B\Lambda\tilde{\theta}_v v(t)$ converges to zero, and hence using (10) and (12), it can be shown that (6) is achieved asymptotically. When $\bar{d} \neq 0$, it can be shown that all the trajectories converge to a compact set E_1. To find E_1, we first introduce two properties of P (Gibson et al., 2015) derived from the Lyapunov equation $A_m^T P + PA_m = -Q$ as

$$\|P\| \leq \chi^2 \|Q\|/\sigma, \tag{A.4}$$

$$\lambda_{\min}(P) \geq \lambda_{\min}(Q)/2s. \tag{A.5}$$

Using (A.1), it follows that

$$\begin{aligned}V &\leq \|e\|^2\|P\| + tr(\tilde{\theta}_v^T \Gamma_\theta^{-1}\tilde{\theta}_v \Lambda) = \|e\|^2\|P\| \\ &+ (1/\gamma_\theta)tr(\tilde{\theta}_v^T\tilde{\theta}_v\Lambda) \leq \|e\|^2\|P\| + (1/\gamma_\theta)\tilde{\theta}_{\max}^2,\end{aligned} \tag{A.6}$$

Since $\theta_v^* \in \hat{\Omega}_{\text{proj}}$, using (A.3) and (3), we have $\dot{V} \leq -\lambda_{\min}(Q)\|e\|^2 + 2\|e\|\|P\bar{d}\|$. By using Young's inequality, it follows that $\dot{V} \leq -\frac{1}{2}\lambda_{\min}(Q)\|e\|^2 + 2\|P\|^2 D^2/\lambda_{\min}(Q)$. Thus, using this inequality and (A.6), we have

$$\begin{aligned}\dot{V}(t) &\leq -\frac{\lambda_{\min}(Q)V}{2\|P\|} + \frac{\lambda_{\min}(Q)\tilde{\theta}_{\max}^2}{2\gamma_\theta\|P\|} + \frac{2\|P\|^2 D^2}{\lambda_{\min}(Q)} \\ &\leq -\omega_1 V + \omega_2,\end{aligned} \tag{A.7}$$

where $\omega_1 = \frac{\sigma\lambda_{\min}(Q)}{2\chi^2\|Q\|}$ and $\omega_2 = \frac{s}{\gamma_\theta}\tilde{\theta}_{\max}^2 + \frac{2\chi^4 D^2\|Q\|^2}{\sigma^2\lambda_{\min}(Q)}$. By using the Gronwall inequality, (A.7) can be rewritten as

$$V(t) \leq \big(V(0) - \frac{\omega_2}{\omega_1}\big)e^{-\omega_1 t} + \frac{\omega_2}{\omega_1}. \tag{A.8}$$

Using $e(t)^T Pe(t) \leq V(t) \leq \big(V(0) - \frac{\omega_2}{\omega_1}\big)e^{-\omega_1 t} + \frac{\omega_2}{\omega_1}$ and taking the limits of the leftmost and rightmost sides as t goes to infinity, we

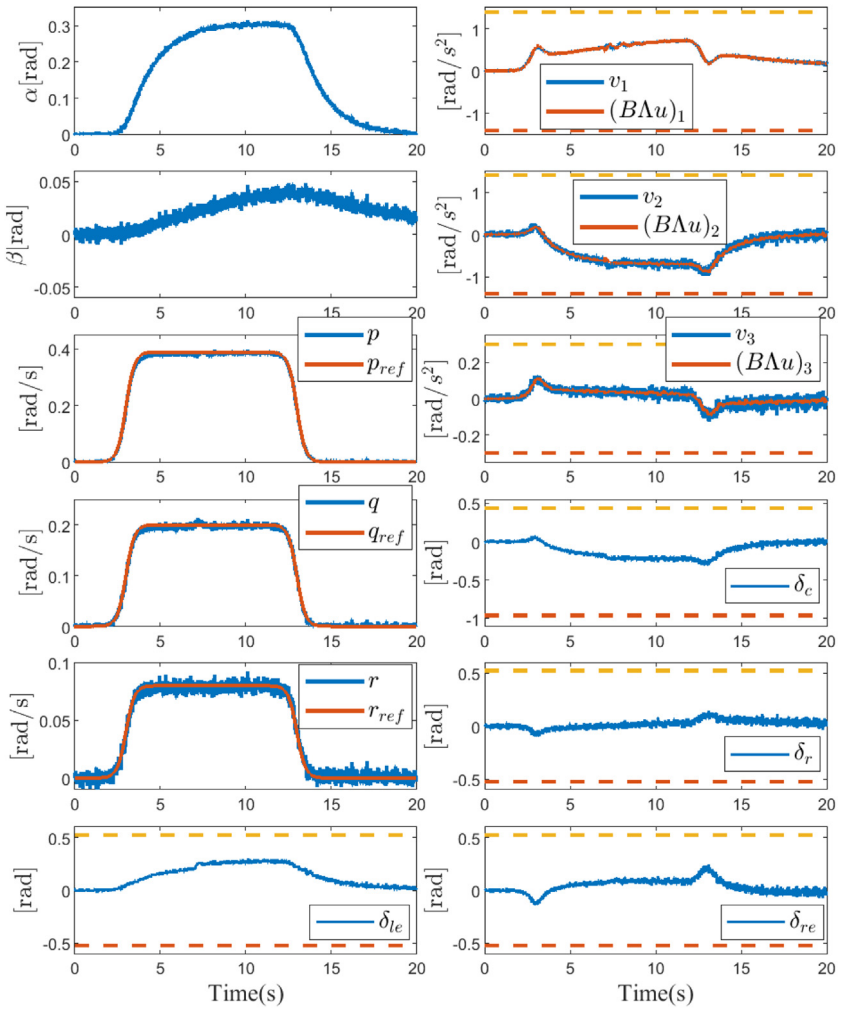

Fig. 4. System states, control signals and actuators' deflections using adaptive control allocation, when actuator loss of effectiveness is 15% after $t = 7$ s.

have

$$\limsup_{t\to\infty} e(t)^T P e(t) \le \left(\frac{s\tilde{\theta}^2_{\max}}{\gamma_\theta} + \frac{2\chi^4 D^2 \|Q\|^2}{\sigma^2 \lambda_{\min}(Q)}\right)\frac{2\chi^2\|Q\|}{\sigma\lambda_{\min}(Q)}. \tag{A.9}$$

By using the inequality $\lambda_{\min}(P)\|e\|^2 \le e^T P e \le \lambda_{\max}(P)\|e\|^2$ and (A.5), we have $\frac{\lambda_{\min}(Q)}{2s}\|e\|^2 \le \lambda_{\min}(P)\|e\|^2 \le e^T P e$. Thus, from (A.9) we have,

$$\limsup_{t\to\infty} \|e(t)\|^2 \le \left(\frac{s\tilde{\theta}^2_{\max}}{\gamma_\theta \lambda_{\min}(Q)} + \frac{2\chi^4 D^2 \|Q\|^2}{\sigma^2 \lambda_{\min}(Q)}\right)\frac{4s\chi^2\|Q\|}{\sigma\lambda_{\min}(Q)}.$$

Therefore, for the initial conditions $e(0)$ and $\theta_v(0) \in \Omega_{\text{proj}}$, $e(t)$ and $\tilde{\theta}_v(t)$ are uniformly bounded for all $t \ge 0$ and system trajectories converge to the compact set E_1 given by (15).

Appendix B. Proof of Lemma 1

For both cases in projection algorithm (1), we have

$$\begin{aligned}
&tr((\theta_v^T - \theta_v^{*T})(-Y + \text{Proj}(\theta_v, Y, f))) \\
&= \sum_{j=1}^{m}\sum_{i=1}^{r}(\theta_{v_{i,j}} - \theta^*_{v_{i,j}})\big(-Y_{i,j} + \text{Proj}(\theta_{v_{i,j}}, Y_{i,j}, f)\big) \\
&\le \sum_{j=1}^{m}\sum_{i=1}^{r}|(\theta_{v_{i,j}} - \theta^*_{v_{i,j}})Y_{i,j} f(\theta_{v_{i,j}})| \le \sum_{j=1}^{m}\sum_{i=1}^{r}|\tilde{\theta}_{i,j}Y_{i,j}| \\
&= tr(|\tilde{\theta}_v^T||Y|) \le \|\tilde{\theta}_v\|_F \|Y\|_F \le \sqrt{r}\tilde{\theta}_{MAX}\|Y\|,
\end{aligned}$$

where we used the property, $\|Y\|_F \le \sqrt{min(r,m)}\|Y\|$, and $|\tilde{\theta}_v^T|$ and $|Y|$ which are the matrices of absolute values of the elements of $\tilde{\theta}_v^T$ and Y, respectively.

Appendix C. Proof of Theorem 2

By using (A.1), (A.3), (17) with $Y = -ve^T PB$, and Young's inequality, we have

$$\dot{V} \le -\frac{1}{2}\|e\|^2 + 4\|P\|^2 D^2 + 4r\tilde{\theta}^2_{MAX}\|P\|^2\|B\|^2 M^2. \tag{C.1}$$

Also, instead of (A.6), we have $\frac{V}{\|P\|} - \frac{\tilde{\theta}^2_{\text{MAX}}}{\gamma_\theta\|P\|} \le \|e\|^2$. Using this inequality, (A.4), (A.5) and (C.1), we obtain

$$\begin{aligned}
\dot{V} &\le -\frac{\lambda_{\min}(Q)V}{2\|P\|} + \frac{\lambda_{\min}(Q)\tilde{\theta}^2_{\text{MAX}}}{2\gamma_\theta\|P\|} + \frac{4\|P\|^2 D^2}{\lambda_{\min}(Q)} \\
&\quad + \frac{4r\tilde{\theta}^2_{\text{MAX}}\|P\|^2\|B\|^2 M^2}{\lambda_{\min}(Q)} \le -\hat{\omega}_1 V + \hat{\omega}_2,
\end{aligned} \tag{C.2}$$

where $\hat{\omega}_1 = \frac{\lambda_{\min}(Q)\sigma}{2\chi^2\|Q\|}$ and $\hat{\omega}_2 = \frac{s\tilde{\theta}^2_{\text{MAX}}}{\gamma_\theta} + 4\frac{\chi^4 D^2\|Q\|^2}{\sigma^2\lambda_{\min}(Q)} + 4\frac{r\tilde{\theta}^2_{\text{MAX}}\chi^4\|B\|^2 M^2\|Q\|^2}{\sigma^2\lambda_{\min}(Q)}$. Following the same procedure as for E_1, $\hat{E}_1$ is obtained and is given by (18).

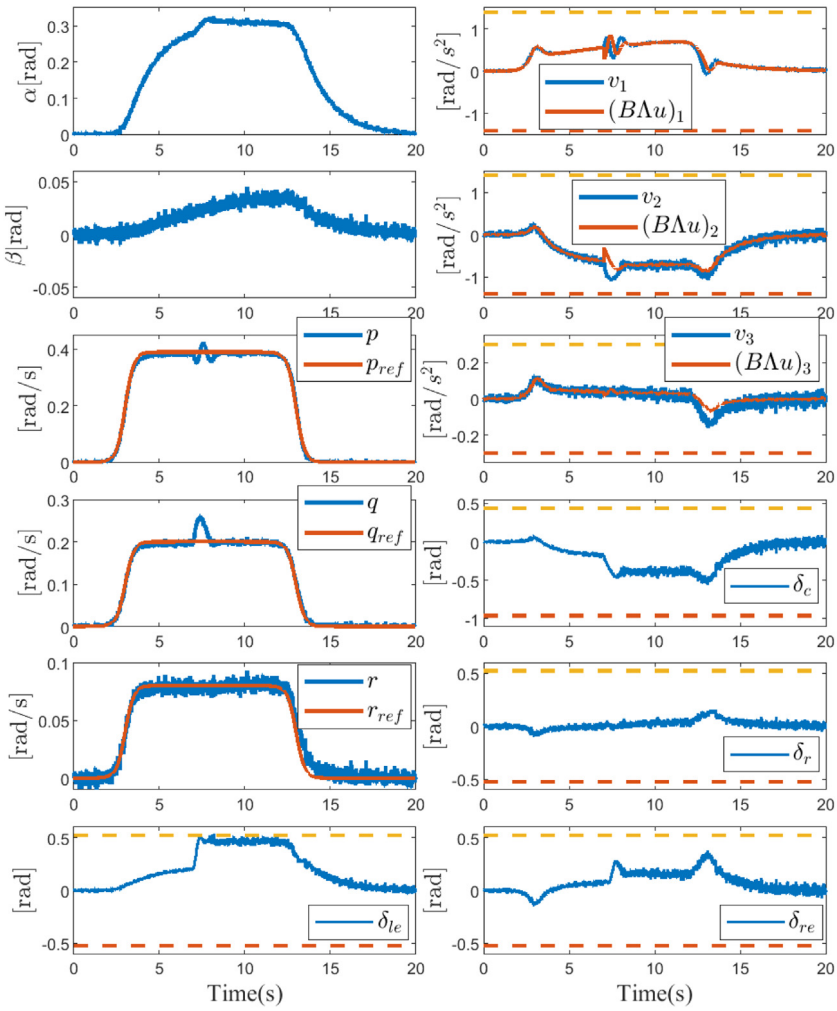

Fig. 5. System states, control signals and actuators' deflections using adaptive control allocation when actuator loss of effectiveness is 50% after $t = 7$ s.

Appendix D. Proof of Theorem 4

To prove the non-emptiness of Υ, we should show that $\| \text{row}_i (B\Lambda\theta_I^{*T} - I_r) \|^2 \leq \frac{M_i^2}{M_{\max}^2} - \epsilon$. Using (26) and the definition of $\theta_I^{*T} = B^T(BB^T)^{-1}$, we have,

$$
\begin{aligned}
&\|\text{row}_i(B\Lambda\theta_I^{*T} - I_r)\|^2 = \|\text{row}_i(B\Lambda B^T(BB^T)^{-1} - I_r)\|^2 \\
&= \|\text{row}_i(B\Lambda B^T(BB^T)^{-1} - BB^T(BB^T)^{-1})\|^2 \\
&\leq \|\text{row}_i(B(\Lambda - I_m))\|^2 \|B^T(BB^T)^{-1}\|^2 \\
&\leq (\lambda_{\max}(\Lambda - I_m))^2 \|\text{row}_i(B)\|^2 \|B^T(BB^T)^{-1}\|^2 \\
&= (\lambda_{\min}(\Lambda) - 1)^2 \|\text{row}_i(B)\|^2 \|B^T(BB^T)^{-1}\|^2. \qquad \text{(D.1)}
\end{aligned}
$$

Therefore, in order to show that $\|\text{row}_i(B\Lambda\theta_I^{*T} - I_r)\|^2 \leq \frac{M_i^2}{M_{\max}^2} - \epsilon$, for all $i = 1, \ldots, r$, we should satisfy

$$
\begin{aligned}
&(\lambda_{\min}(\Lambda) - 1)^2 \|\text{row}_i(B)\|^2 \|B^T(BB^T)^{-1}\|^2 \leq \frac{M_i^2}{M_{\max}^2} - \epsilon \\
&\Rightarrow -\sqrt{\gamma_{M_i}/\gamma_{B_i}} \leq \lambda_{\min}(\Lambda) - 1 \leq \sqrt{\gamma_{M_i}/\gamma_{B_i}}, \ i = 1, \ldots, r,
\end{aligned}
$$

where $\gamma_{B_i} \equiv \|\text{row}_i(B)\| \|B^T(BB^T)^{-1}\|$ and $\gamma_{M_i} = \frac{M_i^2}{M_{\max}^2} - \epsilon$ for all $i = 1, \ldots, r$. Since the maximum value for the diagonal elements of Λ is one, the only condition that should be satisfied is that $1 - \sqrt{\gamma_{M_i}/\gamma_{B_i}} \leq \lambda_{\min}(\Lambda)$ for $i = 1, \ldots, r$ or $\gamma \equiv \max_i(1 - \sqrt{\gamma_{M_i}/\gamma_{B_i}}) \leq \lambda_{\min}(\Lambda)$.

Appendix E. Design procedure

The following procedure can be followed to compute the parameters of our control allocation scheme:

Step 1 — Use Step 1 in Section 4, to determine M_i, $i = 1, \ldots, r$, thus, $\hat{\Omega}_v$ is obtained.

Step 2 — Calculate Ω_θ using Step 2 in Section 4.

Step 3 — Using Theorem 4, calculate $\gamma \equiv \max_i(1 - \sqrt{\gamma_{M_i}/\gamma_{B_i}})$, where $M_{\max} = \max_i M_i$, $\gamma_{M_i} \equiv \frac{M_i^2}{M_{\max}^2} - \epsilon$ for a small positive ϵ, and $\gamma_{B_i} \equiv \|\text{row}_i(B)\| \|B^T(BB^T)^{-1}\|$.

Step 4 — Using γ, obtain $\hat{\Omega}_\Lambda$ in (28).

Step 5 — Solve the optimization problem (25), which leads to obtaining the Ω_{proj}, which is defined in Section 4, Step 3. This allows the implementation of (10).

References

Acosta, D. M., Yildiz, Y., Craun, R. W., Beard, S. D., Leonard, M. W., Hardy, G. H., et al. (2014). Piloted evaluation of a control allocation technique to recover from pilot-induced oscillations. *Journal of Aircraft*, *52*(1), 130–140.

Alwi, H., & Edwards, C. (2008). Fault tolerant control using sliding modes with on-line control allocation. *Automatica*, *44*(7), 1859–1866.

Argha, A., Su, S. W., & Celler, B. G. (2019). Control allocation-based fault tolerant control. *Automatica*, *103*, 408–417.

Bodson, M. (2002). Evaluation of optimization methods for control allocation. *Journal of Guidance, Control, and Dynamics*, *25*(4), 703–711.

Bouarfa, A., Bodson, M., & Fadel, M. (2017). A fast active-balancing method for the 3-phase multilevel flying capacitor inverter derived from control allocation theory. *IFAC-PapersOnLine*, *50*(1), 2113–2118.

Buffington, J. M., & Enns, D. F. (1996). Lyapunov stability analysis of daisy chain control allocation. *Journal of Guidance, Control, and Dynamics*, *19*(6), 1226–1230.

Casavola, A., & Garone, E. (2010). Fault-tolerant adaptive control allocation schemes for overactuated systems. *International Journal of Robust and Nonlinear Control*, *20*(17), 1958–1980.

Chen, M., Ge, S. S., How, B. V. E., & Choo, Y. S. (2013). Robust adaptive position mooring control for marine vessels. *IEEE Transactions on Control Systems Technology*, *21*(2), 395–409.

Corradini, M. L., Cristofaro, A., & Orlando, G. (2010). Robust stabilization of multi input plants with saturating actuators. *IEEE Transactions on Automatic Control*, *55*(2), 419–425.

Cristofaro, A., & Johansen, T. A. (2014). Fault tolerant control allocation using unknown input observers. *Automatica*, *50*(7), 1891–1897.

Cristofaro, A., Polycarpou, M. M., & Johansen, T. A. (2015). Fault diagnosis and fault-tolerant control allocation for a class of nonlinear systems with redundant inputs. In *IEEE conference on decision and control* (pp. 5117–5123).

Demirci, M., & Gokasan, M. (2013). Adaptive optimal control allocation using Lagrangian neural networks for stability control of a 4WS–4WD electric vehicle. *Transactions of the Institute of Measurement and Control*, *35*(8), 1139–1151.

Ducard, G. J. (2009). *Fault-tolerant flight control and guidance systems: Practical methods for small unmanned aerial vehicles*. Springer Science & Business Media.

Durham, W. C. (1993). Constrained control allocation. *Journal of Guidance, Control, and Dynamics*, *16*(4), 717–725.

Durham, W., Bordignon, K. A., & Beck, R. (2009). *Aircraft control allocation*. Springer Science & Business Media.

Edwards, C., Lombaerts, T., Smaili, H., et al. (2010). Fault tolerant flight control. *Lecture Notes in Control and Information Sciences*, *399*, 1–560.

Falconí, G. P., & Holzapfel, F. (2016). Adaptive fault tolerant control allocation for a hexacopter system. In *American control conference (ACC), 2016* (pp. 6760–6766). IEEE.

Galeani, S., & Sassano, M. (2018). Data-driven dynamic control allocation for uncertain redundant plants. In *IEEE conference on decision and control* (pp. 5494–5499).

Gibson, T. E., Qu, Z., Annaswamy, A. M., & Lavretsky, E. (2015). Adaptive output feedback based on closed-loop reference models. *IEEE Transactions on Automatic Control*, *60*(10), 2728–2733.

Gierusz, W., & Tomera, M. (2006). Logic thrust allocation applied to multivariable control of the training ship. *Control Engineering Practice*, *14*(5), 511–524.

Härkegård, O. (2002). Efficient active set algorithms for solving constrained least squares problems in aircraft control allocation. In *IEEE conference on decision and control, Vol. 2* (pp. 1295–1300).

Härkegård, O. (2003). *Backstepping and control allocation with applications to flight control* (Ph.D. thesis), Linköpings universitet.

Härkegård, O., & Glad, S. T. (2005). Resolving actuator redundancy-optimal control vs. control allocation. *Automatica*, *41*(1), 137–144.

Johansen, T. A., & Fossen, T. I. (2013). Control allocation—a survey. *Automatica*, *49*(5), 1087–1103.

Johansen, T. A., Fuglseth, T. P., Tøndel, P., & Fossen, T. I. (2008). Optimal constrained control allocation in marine surface vessels with rudders. *Control Engineering Practice*, *16*(4), 457–464.

Kirchengast, M., Steinberger, M., & Horn, M. (2018). Input matrix factorizations for constrained control allocation. *IEEE Transactions on Automatic Control*, *63*(4), 1163–1170.

Kutay, A., Culp, J., Muse, J., Brzozowski, D., Glezer, A., & Calise, A. (2007). A closed-loop flight control experiment using active flow control actuators. In *45th AIAA Aerospace Sciences Meeting and Exhibit* (p. 114).

Lavretsky, E., & Gibson, T. E. (2011). Projection operator in adaptive systems. arXiv preprint arXiv:1112.4232.

Liao, F., Lum, K.-Y., Wang, J., & Benosman, M. (2010). Adaptive control allocation for non-linear systems with internal dynamics. *IET Control Theory & Applications*, *4*(6), 909–922.

Naderi, M., Sedigh, A. K., & Johansen, T. A. (2019). Guaranteed feasible control allocation using model predictive control. *Control Theory and Technology*, *17*(3), 252–264.

Narendra, K. S., & Annaswamy, A. M. (2012). *Stable adaptive systems*. Courier Corporation.

Petersen, J. A., & Bodson, M. (2006). Constrained quadratic programming techniques for control allocation. *IEEE Transactions on Control Systems Technology*, *14*(1), 91–98.

Podder, T. K., & Sarkar, N. (2001). Fault-tolerant control of an autonomous underwater vehicle under thruster redundancy. *Robotics and Autonomous Systems*, *34*(1), 39–52.

Raoufat, M. E., Tomsovic, K., & Djouadi, S. M. (2017). Dynamic control allocation for damping of inter-area oscillations. *IEEE Transactions on Power Systems*, *32*(6), 4894–4903.

Sadeghzadeh, I., Chamseddine, A., Zhang, Y., & Theilliol, D. (2012). Control allocation and re-allocation for a modified quadrotor helicopter against actuator faults. *IFAC Proceedings Volumes*, *45*(20), 247–252.

Shen, Q., Wang, D., Zhu, S., & Poh, E. K. (2015). Inertia-free fault-tolerant spacecraft attitude tracking using control allocation. *Automatica*, *62*, 114–121.

Shen, Q., Wang, D., Zhu, S., & Poh, E. K. (2017). Robust control allocation for spacecraft attitude tracking under actuator faults. *IEEE Transactions on Control Systems Technology*, *25*(3), 1068–1075.

Sieberling, S., Chu, Q., & Mulder, J. (2010). Robust flight control using incremental nonlinear dynamic inversion and angular acceleration prediction. *Journal of Guidance, Control, and Dynamics*, *33*(6), 1732–1742.

Sørensen, A. J. (2011). A survey of dynamic positioning control systems. *Annual Reviews in Control*, *35*(1), 123–136.

Sørensen, M. E. N., Hansen, S., Breivik, M., & Blanke, M. (2017). Performance comparison of controllers with fault-dependent control allocation for UAVs. *Journal of Intelligent and Robotic Systems*, *87*(1), 187–207.

Stephan, J., & Fichter, W. (2017). Fast exact redistributed pseudoinverse method for linear actuation systems. *IEEE Transactions on Control Systems Technology*, (99), 1–8.

Taghirad, H. D., & Bedoustani, Y. B. (2011). An analytic-iterative redundancy resolution scheme for cable-driven redundant parallel manipulators. *IEEE Transactions on Robotics*, *27*(6), 1137–1143.

Tao, G. (2003). *Adaptive control design and analysis, Vol. 37*. John Wiley & Sons.

Tarbouriech, S., Garcia, G., da Silva Jr, J. M. G., & Queinnec, I. (2011). *Stability and stabilization of linear systems with saturating actuators*. Springer Science & Business Media.

Tjønnås, J., & Johansen, T. A. (2008). Adaptive control allocation. *Automatica*, *44*(11), 2754–2765.

Tjønnås, J., & Johansen, T. A. (2010). Stabilization of automotive vehicles using active steering and adaptive brake control allocation. *IEEE Transactions on Control Systems Technology*, *18*(3), 545–558.

Tohidi, S. S., Khaki Sedigh, A., & Buzorgnia, D. (2016). Fault tolerant control design using adaptive control allocation based on the pseudo inverse along the null space. *International Journal of Robust and Nonlinear Control*, *26*(16), 3541–3557.

Tohidi, S. S., Yildiz, Y., & Kolmanovsky, I. (2016). Fault tolerant control for over-actuated systems: An adaptive correction approach. In *American control conference, 2016* (pp. 2530–2535).

Tohidi, S. S., Yildiz, Y., & Kolmanovsky, I. (2017). *Adaptive control allocation for over-actuated systems with actuator saturation, Vol. 50* (pp. 5492–5497). Elsevier.

Tohidi, S. S., Yildiz, Y., & Kolmanovsky, I. (2018). Pilot induced oscillation mitigation for unmanned aircraft systems: An adaptive control allocation approach. In *IEEE conference on control technology and applications* (pp. 343–348).

Virnig, J., & Bodden, D. (1994). Multivariable control allocation and control law conditioning when control effectors limit. In *Guidance, navigation, and control conference* (p. 3609).

Yang, Y., & Gao, Z. (2020). A new method for control allocation of aircraft flight control system. *IEEE Transactions on Automatic Control*, *65*(4), 1413–1428.

Yildiz, Y., & Kolmanovsky, I. V. (2010). A control allocation technique to recover from pilot-induced oscillations (CAPIO) due to actuator rate limiting. In *American control conference* (pp. 516–523).

Yildiz, Y., & Kolmanovsky, I. (2011a). Implementation of capio for composite adaptive control of cross-coupled unstable aircraft. In *Infotech@ aerospace 2011* (p. 1460).

Yildiz, Y., & Kolmanovsky, I. (2011b). Stability properties and cross-coupling performance of the control allocation scheme CAPIO. *Journal of Guidance, Control, and Dynamics*, *34*(4), 1190–1196.

Yildiz, Y., Kolmanovsky, I. V., & Acosta, D. (2011). A control allocation system for automatic detection and compensation of phase shift due to actuator rate limiting. In *American control conference* (pp. 444–449).

Zaccarian, L. (2009). Dynamic allocation for input redundant control systems. *Automatica*, *45*(6), 1431–1438.

Zhang, Y., & Jiang, J. (2008). Bibliographical review on reconfigurable fault-tolerant control systems. *Annual Reviews in Control*, *32*(2), 229–252.

Seyed Shahabaldin Tohidi received the B.S. degree in Electrical Engineering from Shiraz University of Technology, Shiraz, Iran, in 2010; the M.S. degree in Electrical Engineering from K. N. Toosi University of Technology, Tehran, Iran, in 2014. He is currently a Ph.D. candidate in the Mechanical Engineering Department, Bilkent University, Ankara, Turkey. His current research interests include adaptive control, control allocation, fault-tolerant control, human modeling and human-in-the-loop stability analysis.

Yildiray Yildiz is an assistant professor and the director of the Systems Laboratory at Bilkent University, Ankara, Turkey. He received the B.S. degree (Ranked 1st in class) in mechanical engineering from the Middle East Technical University, Ankara, Turkey, in 2002; the M.S. degree in mechatronics engineering from Sabanci University, Istanbul, in 2004; and the Ph.D. degree in mechanical engineering with a mathematics minor from the Massachusetts Institute of Technology, Cambridge, in 2009. He held postdoctoral associate and associate scientist positions with NASA Ames Research Center, Mountain View, California, from 2009 to 2010, and from 2010 to 2014, respectively. During this time, he was employed by the University of California, Santa Cruz, through its University Affiliated Research Center. He is the recipient of the ASME Best Student Paper in Conference award (2008), the NASA Group Achievement Award (2012) for outstanding technology development, the Turkish Science Academy's Young Scientist Award (2017), the Science Academy, Turkey's Young Scientist Award (2017), and Prof. Mustafa N. Parlar Foundation's Research Incentive Award (2018). He has been serving as an associate editor for IEEE Conference Editorial Board since 2015, IEEE Control Systems Magazine since 2016, European Journal of Control since 2019, and IEEE Transactions on Control Systems Technology since 2020. He has also been a member of the International Journal of Control Editorial Board since 2019. His research interests are the theory and applications of system dynamics and control. He is especially interested in cyber–physical human systems, adaptive control, reinforcement learning and game theory, and applications in the aerospace and automotive domains.

Ilya Kolmanovsky is a professor in the Department of Aerospace Engineering at the University of Michigan. His research interests are in control theory for systems with state and control constraints, and in control applications to aerospace and automotive systems. He received his Ph.D. degree from the University of Michigan in 1995. He is a Fellow of IEEE and is named as an inventor of over a hundred of United States patents.